Proceedings of 8 ICSHMO, Foz do Iguaçu, Brazil, April 24-28, 2006, INPE, p. 1823-1827.

SOUTH-AMERICAN CYCLOGENESIS: PRECURSORS

David Mendes*[1], Enio P. Souza[2], Isabel F. Trigo[1,3], and Pedro M. A. Miranda[1]
University of Lisbon[1], Federal University of Campina Grande[2], Instituto de Meteorologia de Portugal[3]

1. INTRODUCTION

Extra-tropical cyclones play a central role in the maintenance of global climate and are responsible for the transport of heat and moisture through the troposphere (Peixoto and Oort1992; Simmonds and Keay 2000). The South Atlantic is one of the regions of the globe where cyclones preferably occur. According to Frederiksen (1985), the observed location of the primary storm-track just downstream and poleward of the polar jet stream in the southern hemisphere is accounted for by linear baroclinic instability theory. However, James and Anderson (1984), using one of the first years of analyzed data for the Southern Hemisphere, provided by the European Centre for Medium-range Weather Forecasts (ECMWF), found that the linear dry baroclinic theory was unable to explain the observed storm-track in the South Atlantic sector. Gan and Rao (1991) showed that cyclone formation in South America is mostly associated with baroclinic instability. In addition, they pointed out the importance of topographical effects caused by the presence of the Andes Mountains. Furthermore, Garreaud and Wallace (1998) found that transient incursions of mid-latitude air into subtropical and tropical South America, east of the Andes, are an important feature of the synoptic climatology over this region, associated with the enhancement of convection.
This study puts into evidence the conditions which favour the onset and intensification of cyclones in the region of maximum cyclogenesis near South America. It will be shown that events of low-level cyclogenesis are preceded by an increase in the spatial heterogeneity of the moist entropy field, with the buildup of warm and moist air over a preferred South American region, to the North of Argentina.

[1]

2. DATA AND METHODOLOGY

The data used here consist of the following 6-hourly fields, on a 2.5° x 2.5° regular grid: Sea Level Pressure (SLP); 500 hPa geopotential height (Z500); 850 hPa horizontal wind; absolute air temperature and relative humidity, both at 1000 and 500hPa. The data, available from the National Center for Environmental Prediction / National Center for Atmospheric Research (NCEP/NCAR) reanalyses dataset (Kalnay *et al*. 1996), cover the whole Southern Hemisphere (120°W-0°, and 60°S-0°), spanning the period from 1979 to 2003. Cyclones are detected by identifying minimum values in sea level pressure (SLP), according to the methodology proposed by Trigo *et al*. (1999). To be considered a cyclone, these minima must fulfil two empirically defined

[1] Corresponding author address: University of Lisbon, Campo Grande, C8, 8.3.19. Email: dmendes@fc.ul.pt

thresholds: 1) a value not greater than 1020 hPa is required for the system centre in its mature stage; and 2) the mean pressure gradient estimated for an area of 9° lat x 12° long around the centre must be of at least 0.55 hPa/250 km.

The thermodynamic state of the system was analyzed through two variables: the equivalent potential temperature (θ_e) and the saturation equivalent potential temperature (θ_e^*). A detailed description of the calculation of these variables is given by Bolton (1980).

A conditional instability index is used in the following analysis. This is defined as the difference between θ_e at 1000 hPa and θ_e^* at 500 hPa, following Rennó and Ingersol (1996), over the cyclone centre.

Next, the composite means and/or anomalies of this index as well as of SLP, Z500 and near surface wind will be presented and discussed for situations prior, during and after cyclogenesis occurs within the South American maximum shown in Fig. 1, i.e., within the area (70ºW-30ºW; 25ºS-45ºS).

3. RESULTS AND DISCUSSION

Figure 1 shows the winter (JJA) mean number of cyclogenesis near South America. A total of 841 events were diagnosed, from NCEP/NCAR reanalyses, for the period 1979-2003. Most events occur over the Atlantic Ocean, off the Argentinean coast, with some cases in continental South America over Argentina, Uruguay and south Brazil. This result agrees with previous studies (Gan and Rao 1991; Sinclair, 1995; Simmonds and Keay 2000).

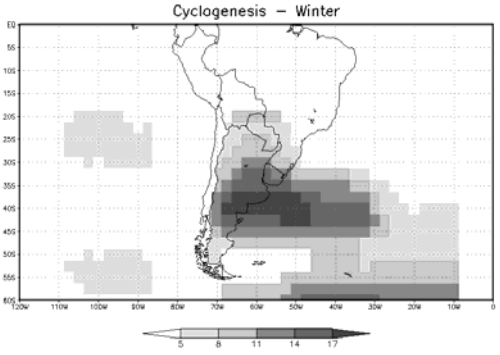

Figure 1 - Spatial distribution of winter (JJA) cyclogenesis around South America. The values correspond to the average number of events per JJA season, detected per 5º × 5º gird-cells.

Figure 2 displays the JJA mean distribution of 850 hPa wind and 1000 hPa θ_e and θ_e variance. As previously mentioned, it displays important meridional low level flow on both sides of the Andes mountains. The region of maximum θ_e lies east of the Andes, extending southwards along the northerly warm and moist flow from the Amazon basin, i.e. the low level jet (Marengo *et al*. 2004).

The region of maximum θ_e variance is much further to the south, centred near 25ºS, 60ºW, over Argentina, and coincides with a region where extratropical cyclones (Gan and Rao 1991; Satyamurty *et al*. 1998). The high variance over latitudes south of 60ºS marks the mean position of the circumpolar winter storm tracks (e.g., Simmonds and Keay 2000).

The fact that the region of most frequent cyclogenesis (Fig. 1) is located slightly to the south of the region of maximum θ_e variance suggests a link between the buildup up of anomalous θ_e in the continent and the process of cyclogenesis that will now be explored.

Figs. 3(a)-3(f) show composite anomalies, with respect to the 1979-2003 winter climatology, of SLP and 500 hPa geopotential height (upper panels), and of the 850 hPa mean flow and 1000 hPa θ_e (lower panels), corresponding to the pre-storm formation (day -1), cyclogenesis (day 0) and post storm formation (day +1). The statistical significance of the anomaly fields is evaluated using a two-tailed Student's t-test (e.g., Wilks, 1995).

Composites of Z500, for the days preceding cyclogenesis in South America, show a moving trough over the South-Eastern Pacific, already centred over the Southern tip of the Andes barrier at day-1 (Fig. 3(a)). The mean location of the trough aloft, which is generally associated with a travelling low originated over the South Pacific, does not change much throughout the year, being generally within the 40ºS-50ºS band. A slightly negative, but significant, SLP anomaly over South America is present in the composite fields from day-1 (Fig. 3a), onwards. However, the visual inspection of SLP charts for 24 winter seasons has revealed that these negative anomalies

correspond to a closed isobar at the surface in only 2% of the cases; as expected, in those 2% events, the pressure gradient is still very weak, and does not pass the cyclone detection criterion (section 2).

As the upper perturbation moves over the Andes in the day before cyclone formation, the maximum θ_e anomaly is centred at 30ºS, 60ºW (Fig. 3(b)) and intensifies up to 8K at day 0 (Fig. 3(d)), in the same location. The wind anomalous field at day -1 exhibits enhanced northerly flow over most of the continent, particularly along the eastern flank of the Andes (Fig. 3(b)) transporting tropical moist air southeastwards into the preferred cyclogenetic sector. At day 0 (Fig. 3(d)) the anomalous flow turns to southerly for latitudes to the south of 25ºS in the west part of the Continent, intensifying the low level convergence in the region of maximum θ_e anomaly. At day +1 the maximum θ_e anomaly is reduced and advected to the ocean (Fig. 3(f)). At days 0 and +1 there is clear evidence of a developing cyclonic circulation near the coast (Figs. 3(d) and 3(f)) superimposed over the area of negative SLP anomalies (Figs. 3(c) and 3(e)), in agreement with Fig. 1.

Results shown in Figs. 2 and 3 suggest that the southward transport of moist entropy from tropical Amazon into the subtropics and to the mid-latitude east coast of South America is an essential feature associated with cyclogenesis in this sector. The composite fields analysed here suggest cyclogenesis in the South American Region is generally associated with (i) the accumulation of moist entropy in the continent (Fig.3(d)), well to the south of its mean location (Fig. 2), and (ii) the propagation of an upper-level trough over the Southern tip of the Andes barrier. The latter favours the formation a cyclonic cell in the lee side, over the area of enhanced warm moist air near the coast of Argentina, with low-level convergence intensified by an anomalous southerly flow at higher latitudes.

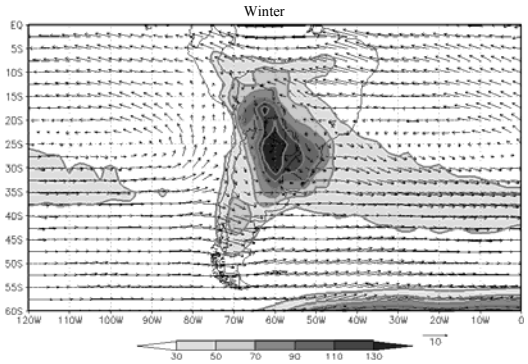

Figure 2 - Winter (JJA) climatological mean variance (shaded; K^2) of equivalent potential temperature at 1000 hPa, computed for the 1979-2003 period. The arrows represent the mean wind vector (ms^{-1}) at 850 hPa, for the same period.

The evolution of the selected thermodynamic properties to the storm development will now be analyzed. Figure 4 shows, for each season (JJA, SON, DJF, and MAM, respectively), composite means of the evolution of the cyclone central pressure (δp), measured as the difference between the cyclone central pressure at time *t* and at the formation time *t=0*), the potential temperature anomaly in the region of maximum variance over South America (30ºS, 60ºW), and the conditional instability index at the cyclone center (difference between 1000 hPa equivalent potential temperature $\theta_{e\ 1000}$, and 500 hPa saturation equivalent potential temperature, $\theta^*_{e\ 500}$). Some remarkable features are present in all seasons, namely: (i) the potential temperature anomaly in the region of maximum variance (30ºS, 60ºW) peaks at the cyclone formation time (*t=0*), while (ii) the conditional instability index ($\theta_{e1000} - \theta^*_{e500}$) increases after the formation of the cyclone, peaking in its mature state, 36 or 48 hours after cyclogenesis. The conditional instability index behaves somewhat differently throughout the year. Spring and autumn show similar curves, with a large increase of the index after the formation of the cyclone. In summer, the conditional instability index is already large at cyclogenesis, and attains an even higher value afterwards. In winter the index is much weaker and hardly responds to the cyclone cycle. In winter, the pressure in the centre of the mean cyclone deepens for about 48 h, whereas in the remaining

seasons deepening is observed for about 72 h. However, the mean deepening is comparable in all seasons, around 8 hPa peak-to-peak.

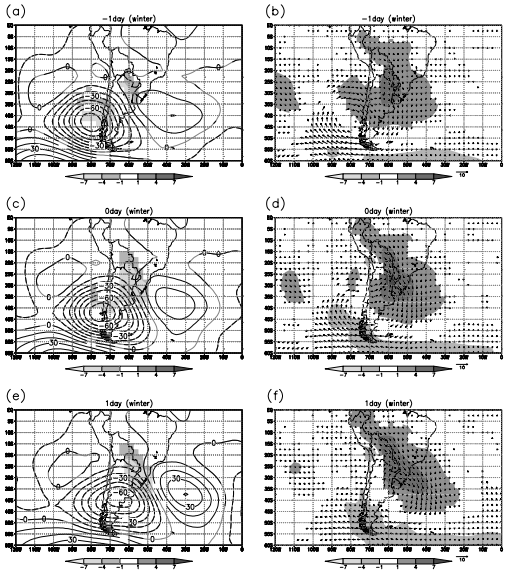

Figure 3 - Upper panels show anomalies of 500 hPa geopotential height (contours every 15 gpm; thick lines correspond to significant anomalies at less than 5%), and of SLP (shaded fields in hPa, showing only anomalies significant at less than 5%), for (a) 1 day before, (c) during , and (e) 1 day after cyclogenesis. The same holds for panels (b), (d) and (f), for anomalies of 850 hPa wind (arrows; ms^{-1}) and 1000 hPa equivalent potential temperature (shaded in K); only significant anomalies (p < 5%) are shown.

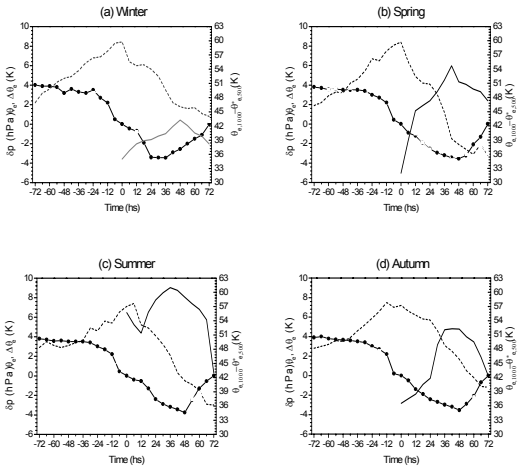

Figure 4 – Pressure at the cyclone centre, δp , minus its value at cyclogenesis (circles; for t<0, the value corresponds to the cyclone formation position), anomaly of 1000 hPa equivalent potential temperature ($\theta_e^{'}$) at 30ºS/60ºW (dashed line), and the conditional instability index (θ_e at 1000-hPa minus θ_e^* at 500-hPa at the cyclone centre; thick solid line, for t>0), for: (a) winter (JJA), (b) spring (SON), (c) summer (DJF), and (d) autumn.

4. CONCLUDING REMARKS

This study is focused on the analysis of preconditions for the formation of South American extratropical cyclones, particularly of low-level thermodynamic variables The winter climatology shows a large space and time variability of near-surface moist entropy, which also holds true for to the remaining seasons. Nevertheless, its distribution is such that there is always a high-entropy reservoir northwest of the cyclone formation region. During the pre-formation period, when a tendency of pressure lowering in the formation region is already noted, there is an increased convergence of moist air into Northern Argentina, northwest of the cyclogenetic region, leading to large positive anomalies in the moist entropy field (θ_e).

On average, for all seasons, this anomaly reaches its maximum at the time of cyclogenesis. After that time, the anomaly decays rapidly, as the newly formed cyclone advects moist air eastwards. In the first day after cyclone formation, while the system deepens and evolves to its mature stage, an anomalous southerly flow of colder air (latitudes 25ºS-40ºS over South America; Fig. 3(f)) may contribute to its development.

The increase in conditional instability after cyclogenesis is due to supply of moist warm air to the cyclogenetic region from the continent, which is turned off as the storm evolves and induces an anomalous southerly flow in the region, reducing the moist entropy anomaly in the continent. Composites of 500 hPa height exhibit a deep trough located to the west of the Andes on day –1, consistent with the analysis of Seluchi (1995), which moves eastwards in the following days. The surface cyclone over the South American Region forms as the upper trough passes the Andes mountain barrier, with the consequent gain of cyclonic circulation on the lee side, being further fuelled by the existing surface θ_e reservoir.

In conclusion, the mid-latitude cyclones that are produced in the Southern South American Region are largely controlled by

interactions between the mid-latitude circulation and the tropics, through north-south flow over the continent, along the east slope of the Andes Mountains. The mean circulation in the region, reinforced in the days prior to cyclogenesis, transports moist air from the Amazon basin into east subtropical South America, near 15ºS 70ºW, very close to the Andes.

ACKNOWLEDGMENTS

The present work was supported by the Portuguese Foundation for Science and Technology, Grants BD/8482/2002 and POCTI/CTA/46573/2002, co-financed by the EU through program FEDER.

REFERENCES

Bolton, D. 1980. The computation of equivalent potential temperature, *Mon. Wea. Rev*., 7, 1046-1053.

Emanuel, K.A. 1989. The finite-amplitude nature of tropical cyclogenesis, *J. Atmos. Sci.,* 46, 3431-3456.

Frederiksen, J.S., 1985. The Geographical Locations of Southern Hemisphere Storm Tracks: Linear Theory. *J. Atmos. Sci.* 42, 710–723.

Gan, M. A., and Rao, V. B. 1991. Surface cyclogenesis over South America. *Mon. Wea. Rev*., 119, 1293-1302.

Garreaud, R.D. and Wallace, J. M. 1998. Summertime incursions of midlatitude air into subtropical and tropical South America, *Mon. Wea. Ver*., 10, 2713-2733.

James, I. N. and Anderson, D.,L.,T., 1984. The seasonal mean flow and distribution of large-scale weather systems in the southern hemisphere: the effects of moisture transports. *Quart. J. R. Met. Soc*., 110, 943-966.

Kalnay, E. and Coauthors 1996. NCEP/NCAR 40-year reanalysis project, *Bull. Am. Meteorol. Soc.*, 77, 437-471.

Marengo, J. A., Soares, W. R., Saulo, C. and Nicolini, M. 2004. Climatology of the Low-Level Jet east of the Andes as derived from the NCEP reanalyses, J. Climate, 17, 2261-2280.

Peixoto, J. P. and Oort, A. H. 1992. *Physics of Climate*, American Institute of Physics, New York, 520 pp.

Rennó, N. O. and Ingersoll, A. P. 1996. Natural convection as a heat engine: A theory for CAPE, *J. Atmos. Sci.,* 53**,** 572-585.

Satyamurty, P., Nobre, C. A. and Silva Dias, P. L. 1998. Meteorology of the tropics. South America. pp 119-139, *in Meteorology of the Southern Hemisphere.* Eds. D. K. Karoly and D. G. Vincent. Meteorological Monographs, 49, American Meteorological Society', Boston.

Seluchi, M.E. 1995. Diagnostico y prognostico de situaciones sinopticas conducentes a cyclogenesis sobre el este de Sudamerica*, Geofisica Internacional*, 34, 171-186.

Sinclair, M. F. 1995. A climatology of cyclogenesis for the Southern Hemisphere, *Mon. Wea. Rev*., 123, 1601-1619.

Simmonds, I. and Keay, K. 2000. Mean southern hemisphere extratropical cyclone behavior in the 40-year NCEP-NCAR reanalysis, *J. Climate*, 13, 873-885.

Trigo I.F., Davies, T. D. and Bigg, G. R. 1999. Objective climatology of cyclones in the Mediterranean region, *J. Climate*, 12, 1685-1696.

Velasco, I. and Fritsch, M. 1987. Mesoscale convective complexes in Americas, *J. Geophys. Res*., 92, 9591-9613.

Wilks, D., 1995. Statistical Methods in the Atmospheric Sciences. An Introduction. Academic Press, San Diego, 467pp.